SCIENTIFIC REPORTS

OPEN

SUBJECT AREAS:
RECOMBINANT PROTEIN THERAPY
ANTIBODY FRAGMENT THERAPY
RECOMBINANT PEPTIDE THERAPY

Received
27 October 2014

Accepted
26 November 2014

Published
17 December 2014

Correspondence and requests for materials should be addressed to J.L. (lofblom@kth.se)

Simultaneous targeting of two ligand-binding sites on VEGFR2 using biparatopic Affibody molecules results in dramatically improved affinity

Filippa Fleetwood[1], Susanne Klint[2], Martin Hanze[1], Elin Gunneriusson[2], Fredrik Y. Frejd[2,3], Stefan Ståhl[1] & John Löfblom[1]

[1]Division of Protein Technology, School of Biotechnology, KTH - Royal Institute of Technology, AlbaNova University Center, 106 91 Stockholm, Sweden, [2]Affibody AB, Gunnar Asplunds Allé 24, 171 63 Solna, Sweden, [3]Unit of Biomedical Radiation Sciences, Uppsala University.

Angiogenesis plays an important role in cancer and ophthalmic disorders such as age-related macular degeneration and diabetic retinopathy. The vascular endothelial growth factor (VEGF) family and corresponding receptors are regulators of angiogenesis and have been much investigated as therapeutic targets. The aim of this work was to generate antagonistic VEGFR2-specific affinity proteins having adjustable pharmacokinetic properties allowing for either therapy or molecular imaging. Two antagonistic Affibody molecules that were cross-reactive for human and murine VEGFR2 were selected by phage and bacterial display. Surprisingly, although both binders independently blocked VEGF-A binding, competition assays revealed interaction with non-overlapping epitopes on the receptor. Biparatopic molecules, comprising the two Affibody domains, were hence engineered to potentially increase affinity even further through avidity. Moreover, an albumin-binding domain was included for half-life extension in future *in vivo* experiments. The best-performing of the biparatopic constructs demonstrated up to 180-fold slower dissociation than the monomers. The new Affibody constructs were also able to specifically target VEGFR2 on human cells, while simultaneously binding to albumin, as well as inhibit VEGF-induced signaling. In summary, we have generated small antagonistic biparatopic Affibody molecules with high affinity for VEGFR2, which have potential for both future therapeutic and diagnostic purposes in angiogenesis-related diseases.

Angiogenesis is the formation of new blood vessels, which is an essential process in growth and development as well as in wound healing[1,2]. However, it is also a key step in tumor development[3] and important in several other diseases, such as age-related macular degeneration of the eye and diabetic retinopathy[4]. Some of the main regulators of angiogenesis are the members of the vascular endothelial growth factor (VEGF) protein family, including VEGF-A, VEGF-B, VEGF-C, VEGF-D and placental growth factor (PlGF)[1,2,5]. The receptors that mediate the angiogenic activities of these ligands include VEGF receptor 1 (VEGFR1), VEGFR2 and VEGFR3[1]. VEGFR2 plays the most important role in angiogenesis, and is activated by different isoforms of VEGF-A, -C, and -D. The extracellular domain of the receptors consists of seven Ig-homology domains, of which domains 2 and 3 contain the ligand-binding site[6]. Binding of the dimeric VEGF to VEGFR2 mediates receptor dimerization, which induces phosphorylation of the intracellular kinase domains and activates downstream signaling pathways resulting in endothelial cell proliferation, cell migration and vascular permeability[2].

A number of therapeutic strategies have been developed to interfere with angiogenesis[2]. Examples include small molecules acting as antagonists[7,8], or inhibiting the tyrosine kinase signaling[9,10], as well as monoclonal antibodies and fusion proteins targeting the VEGF ligands and receptors[2]. However, although several agents are in the clinic[11,12], lack of response in some patients, and development of resistance has been observed[2,13]. In order to quickly identify such problems, better biomarkers and diagnostic tools are needed[14]. IMC-1121B (Ramucirumab, ImClone Systems)[15,16] is a human anti-VEGFR2 mAb, which was approved by the FDA in 2014 as a treatment for advanced gastric cancer (www.clinicaltrials.gov). Targeting of the receptor rather than the ligand is potentially preferable, since activation of the receptor by other species of VEGF (VEGF-C and –D) is also inhibited[11].

VEGFR2 is also a promising target for *in vivo* imaging of angiogenesis, which can be used as a companion diagnostic tool for monitoring response as well as distinguishing responders from non-responders to various therapies[14,17–19]. However, mAbs are in general unsuitable for molecular imaging due to their very long circulation time in blood, which results in poor contrast[20]. Still, monoclonal antibodies are the traditional affinity proteins for targeted therapeutics. In for example oncology, the Fc-mediated effects often result in important mechanisms of action, such as ADCC and complement activation. However, in therapeutic applications aimed at blocking a protein/protein interaction for inhibition of for example signaling, the large and relatively complex mAb format is not necessarily required. Numerous studies have reported that much smaller affinity proteins based on non-immunoglobulin scaffolds can be engineered for extremely high affinity and specificity[21,22]. Moreover, such alternative scaffolds have typically many additional valuable properties compared to antibodies. Development of VEGFR2-specific Nanobodies have recently been reported[23] and an Adnectin denoted CT-322 (based on a protein scaffold derived from the 10th type III of human fibronectin), targeting human and murine VEGFR2, showed promising results in Phase I clinical trials[24] and is currently in Phase II clinical trials (www.clinicaltrials.gov). Affibody molecules are a class of alternative scaffold proteins that have been thoroughly investigated for both therapeutic and diagnostic applications[25]. A HER2-specific Affibody molecule is currently evaluated in the clinic for molecular imaging of breast cancer[26] and an Affibody-based inhibitor of complement protein C5 entered phase I clinical trials in 2014 (http://clinicaltrials.gov). Affibody molecules are around 6.5 kDa and are efficiently produced in prokaryotic hosts as well as by chemical peptide synthesis. The sequence is devoid of disulphides, and unique cysteines can be incorporated for site-directed conjugation of various compounds, such as cytotoxic payloads. The fast and independent folding of the small domain makes engineering of various multimer formats relatively straightforward. The small size also results in improved tissue penetration as well as rapid renal clearance, leading to excellent contrast in molecular imaging[27–30]. For therapy, several strategies are available for prolonging the half-life in the circulation, including an in-house developed approach of fusing a small albumin-binding domain for non-covalent association to serum albumin. Depending on the format, the same Affibody molecule might hence be used for both diagnostic and therapeutic purposes. Taken together, the properties of Affibody molecules are well suited for targeting of angiogenesis.

In this study, we selected two antagonistic and cross-reactive anti-VEGFR2 Affibody molecules with phage display. Interestingly, competition experiments revealed that the candidates targeted two non-overlapping epitopes on VEGFR2. We used an in-house developed bacterial display method and FACS for affinity maturation of both binders. To potentially increase the affinity even further, we engineered new biparatopic Affibody molecules. Our hypothesis was that if the two domains were able to bind simultaneously to a single receptor molecule, the dimeric construct might result in even higher affinity by an avidity effect that would be independent of receptor density. The new biparatopic format was successful and the heterodimer demonstrated an off-rate that was around two orders of magnitude slower compared to the monomeric binders. We also included an albumin-binding domain (ABD) in the fusion protein, which might be used for extending the circulatory half-life in future in vivo studies. Biosensor assays demonstrated that the biparatopic Affibody molecules, comprising ABD, indeed could bind the receptor while simultaneously interacting with human serum albumin. The Affibody molecules were also able to target VEGFR2 on human 293/KDR cells and inhibit VEGF-A induced phosphorylation. We believe they have potential for both future therapeutic purposes (as fused to ABD for long residence in the circulation) and diagnostic purposes (as non-ABD fused for rapid clearance and improved imaging contrast), in cancer as well as in ophthalmic diseases.

Results

Phage display selection and screening of binders to VEGFR2. An Affibody library displayed on M13 filamentous phage was used to select binders to human VEGFR2. After four selection rounds, candidate clones were analyzed using ELISA for binding to the receptor. Two clones binding to both human and murine VEGFR2 were identified and denoted Z_{VEGFR2_1} and Z_{VEGFR2_2}, respectively. Comparison of the sequences of these two variants revealed a low level of similarity, indicating that the two Affibody molecules might be interacting with different epitopes on VEGFR2 (Supplementary Table S1).

Specificity and epitope analysis. The specificity of the two VEGFR2-binding clones was analyzed using ELISA. Both clones showed binding to human and murine VEGFR2, but not to the closely related receptors VEGFR1 and VEGFR3 (Supplementary Fig. S1). Next, we analyzed if the selected binders were recognizing an epitope that was overlapping with the binding site of VEGF-A. Human or murine VEGFR2 was pre-incubated with a 15-fold molar excess of human VEGF-A. Pre-incubation dramatically reduced the signal for both variants (Supplementary Fig. S1), indicating that the Affibody molecules recognized the same or a partially overlapping binding site as VEGF-A.

Analysis of heat stability and refolding of VEGFR2-binding Affibody molecules. The genes encoding Z_{VEGFR2_1} and Z_{VEGFR2_2} were subcloned into an expression vector for production of soluble proteins. Proteins were purified by IMAC and eluates were analyzed using SDS-PAGE, demonstrating single bands of correct length with no detectable contaminants (data not shown). The heat stability and refolding capacity of Z_{VEGFR2_1} and Z_{VEGFR2_2} was analyzed using circular dichroism (CD) spectroscopy. Both Affibody molecules had an alpha-helical content that was similar to previously reported binders and refolded after heat-induced denaturation at 91°C. Melting temperatures were estimated to around 45°C for Z_{VEGFR2_1} and around 50°C for Z_{VEGFR2_2} (Supplementary Fig. S2).

Affinity determination of VEGFR2-binding Affibody molecules. The kinetics of the binding of the two Affibody molecules to human and murine VEGFR2 were analyzed in a surface plasmon resonance (SPR)-based biosensor assay. Binding of Z_{VEGFR2_1} and Z_{VEGFR2_2} to human and murine VEGFR2 was detected by injecting the Affibody molecules over human or murine VEGFR2, immobilized on the chip surface. Data was fitted using non-linear regression to a monovalent binding model and the equilibrium dissociation constants (K_D) were calculated from the obtained association and dissociation rates to 162 $\pm$ 19 nM for Z_{VEGFR2_1} and 78 $\pm$ 0 nM for Z_{VEGFR2_2} for human VEGFR2, as well as to 258 $\pm$ 22 nM for Z_{VEGFR2_1} and 91 $\pm$ 18 nM for Z_{VEGFR2_2} for murine VEGFR2 (Fig. 1a; Supplementary Fig. S3).

SPR-based competition assays. An SPR-based approach was used to investigate whether Z_{VEGFR2_1} and Z_{VEGFR2_2} could bind simultaneously to the receptor. First, a saturating concentration of Z_{VEGFR2_1} was injected over immobilized human or murine VEGFR2, directly followed by an injection of a mix of Z_{VEGFR2_1} and Z_{VEGFR2_2} or only Z_{VEGFR2_1} for comparison. A substantial additional increase in response signal was observed for the mix, but not for Z_{VEGFR2_1} alone (Fig. 1b). The experiment was also conducted in the reverse order, and again, there was a large increase in signal upon the second injection of Z_{VEGFR2_1} and Z_{VEGFR2_2} (Supplementary Fig. S4). The experiments were also repeated using murine VEGFR2, resulting in a similar response (Supplementary Fig. S4). The results demonstrated that Z_{VEGFR2_1} and Z_{VEGFR2_2} were able to bind simultaneously to VEGFR2 and,

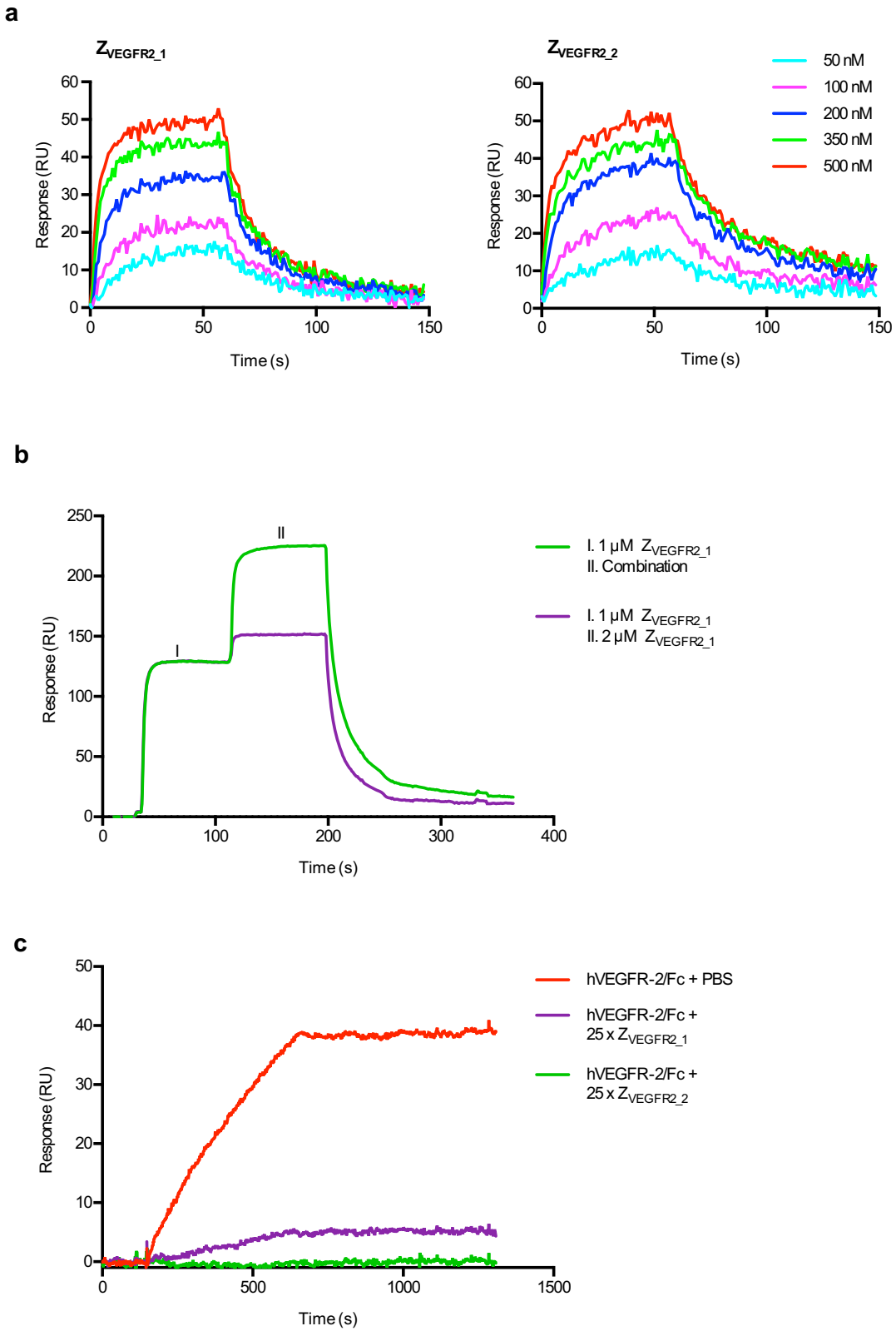

Figure 1 | Characterization of VEGFR2-binding Affibody molecules from phage display selection. (a) Sensorgrams from SPR analysis of Z_{VEGFR2_1} and Z_{VEGFR2_2} binding to immobilized human VEGFR2. Affibody molecules were injected at concentrations ranging from 50 nM to 500 nM. Data is double referenced by subtraction of simultaneous responses from reference surface and a buffer injection. The experiment was performed in duplicates. (b) Representative results from SPR-based competition assay. Sensorgrams were obtained from a double injection, where a first injection of 1 μM of Z_{VEGFR2_1} (I) was immediately followed by a second injection (II) of either a combination of 1 μM of Z_{VEGFR2_1} and 1 μM of Z_{VEGFR2_2}, or 2 μM of Z_{VEGFR2_1}, over immobilized human VEGFR2. The experiment was performed in duplicates. (c) Representative results from SPR-based analysis of human VEGF blocking. 40 nM of human VEGFR2, which had been pre-incubated for 40 min with a 25 × molar excess of Z_{VEGFR2_1}, Z_{VEGFR2_2} or PBS (control), was injected over a surface of immobilized human VEGF-A. The experiment was performed in duplicates.

consequently, that the Affibody molecules interacted with distinct and non-overlapping epitopes on VEGFR2.

Moreover, an additional SPR-based competition experiment was conducted to verify the results from the ELISA, which indicated that the Affibody molecules competed with VEGF-A for binding to VEGFR2. Human and murine VEGFR2 was preincubated with Z_{VEGFR2_1}, Z_{VEGFR2_2} or PBS, respectively, and injected over surfaces with immobilized human and murine VEGF-A, respectively. Injection of the control sample, containing VEGFR2 preincubated with PBS, resulted in an increase in signal, as expected (Fig. 1c). Injection of the samples containing VEGFR2 preincubated with the Affibody molecules resulted in a dramatically lower response, showing that the Affibody molecules blocked the interaction between VEGFR2 and VEGF-A (Fig. 1c). The experiments were also repeated using murine VEGFR2, demonstrating similar results (Supplementary Fig. S5).

Alanine scanning of VEGFR2-binding Affibody molecules Z_{VEGFR2_1} and Z_{VEGFR2_2}. With the aim to increase the affinity of Z_{VEGFR2_1} and Z_{VEGFR2_2} for VEGFR2, a combinatorial-based affinity maturation strategy using display on the surface of *S. carnosus* was applied. First, alanine scanning mutagenesis was used to analyze the individual contributions from 13 residues (same positions as randomized in the library) in the Affibody molecules Z_{VEGFR2_1} and Z_{VEGFR2_2} to the interaction with VEGFR2. The 26 mutants were expressed and displayed on the surface of staphylococci and binding to VEGFR2 was analyzed by flow cytometry (Fig. 2). For Z_{VEGFR2_1}, the majority of the mutations

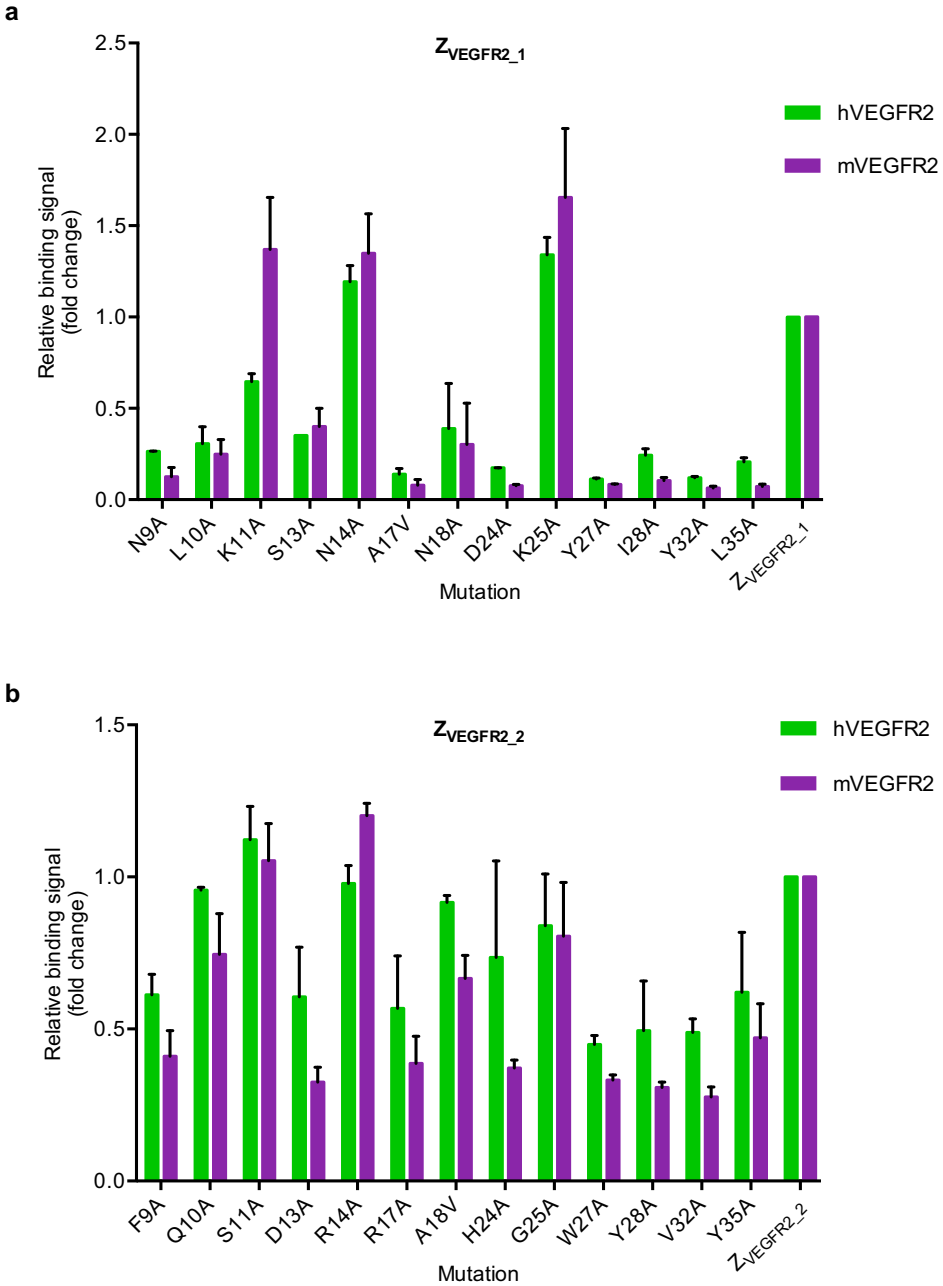

Figure 2 | Alanine scanning of first-generation VEGFR2-specific Affibody molecules. (a) Z_{VEGFR2_1} (b) Z_{VEGFR2_2}. The 13 residues in the VEGFR2-binding Affibody molecules that were substituted with alanine are represented on the X axis, and the fold change in normalized binding signal (a ratio of FL-1 fluorescence intensity, corresponding to VEGFR2 binding, and FL-6 fluorescence intensity, corresponding to surface expression level) compared to the corresponding non-mutated binder (Z_{VEGFR2_1} or Z_{VEGFR2_2}) is represented on the Y axis. Binding to human (green bars) or murine (purple bars) VEGFR2 is shown. The error bars show the standard deviation of two independent experiments.

lead to a substantial decrease in VEGFR2 affinity, indicating that these positions were important for VEGFR2-binding. Three positions (position 11, 14 and 25), were not affected or showed an increased binding signal when mutated to alanine. For Z_{VEGFR2_2}, the effect of the mutations varied more among the positions. Mutations in position 10, 11, 14, 18 and 25 had the smallest effect on the binding.

Design and construction of affinity maturation libraries. Two affinity maturation libraries were designed, and the mutation frequency in each position was based on the results from the alanine scan of Z_{VEGFR2_1} and Z_{VEGFR2_2}, in principle as previously described by Malm *et al.*[21]. Briefly, each selected position was randomized with 18 codons corresponding to all amino acids except cysteine and proline. The original amino acid residues from the sequences of the VEGFR2 binders Z_{VEGFR2_1} and Z_{VEGFR2_2} were included at a higher proportion, in order to generate an average mutation frequency of approximately three mutations per molecule. The randomization frequency in each position was also normalized with the results from the alanine scan, resulting in a lower degree of mutation in positions important for VEGFR2 binding and a higher degree of mutation in positions of less importance (Table 1 and 2). The libraries of DNA fragments were subcloned into the staphylococcal display vector and transformed into *S. carnosus* generating a diversity of approximately 4×10^7 individual transformants for each library. Sequence analysis of individual library members verified a distribution of codons in accordance with the theoretical design (data not shown).

Selection of affinity-matured VEGFR2-specific Affibody molecules using FACS. Fluorescence-activated cell sorting (FACS) was used for isolation of staphylococcal cells displaying Affibody molecules with increased affinity for VEGFR2. Four rounds of sorting was performed, using a starting concentration of 50 nM human VEGFR2, and decreasing to 20 nM in the third round (Fig. 3). Surface expression level was monitored using fluorescently labeled HSA as described previously[31]. In the fourth sorting round, an off-rate selection strategy was applied. The bacterial displayed library was incubated with 50 nM of labeled VEGFR2, followed by washing and incubation for 30 min or 4.5 h with an excess of unlabeled VEGFR2 to minimize rebinding of dissociated labeled target. In addition to the off-rate selection in the last round, the selection stringency was also increased throughout the four sorting rounds by using more stringent gating and sorting parameters. Sequencing of the isolated output identified 50 unique variants from $Z_{VEGFR2\_1matlib}$, and 17 unique variants from $Z_{VEGFR2\_2matlib}$. Interestingly, all except three variants from $Z_{VEGFR2\_2matlib}$ contained a mutation in a non-randomized position (K33N). Position 11, 14 and 25 were the most frequently mutated in the output from $Z_{VEGFR2\_1matlib}$, which was in agreement with the alanine scan data. Position 11 was the most frequently mutated position in the output from $Z_{VEGFR2\_2matlib}$. The average number of mutated amino acids among the selected clones was 2.9 from $Z_{VEGFR2\_1matlib}$, and 2.1 from $Z_{VEGFR2\_2matlib}$, thus also in good agreement with the library design.

On-cell affinity ranking of second-generation VEGFR2-specific Affibody molecules. The binding of individual variants to human VEGFR2 was compared by flow-cytometric analysis of recombinant staphylococci. The 22 most frequently abundant binders from $Z_{VEGFR2\_1matlib}$, and the 17 unique binders from $Z_{VEGFR2\_2matlib}$ were included in the assay (Supplementary Fig. S6). In order to obtain a ranking influenced by the off-rates, the samples were subjected to 30 min or 4.5 h incubations with unlabeled VEGFR2 after incubation with labeled target. All analyzed clones showed slower dissociation compared to the original binders Z_{VEGFR2_1} and Z_{VEGFR2_2}. The top ten binders from $Z_{VEGFR2\_1matlib}$ and the top eight binders from $Z_{VEGFR2\_2matlib}$ were also analyzed using murine VEGFR2, showing retained cross-reactivity to murine VEGFR2 (Supplementary Fig. S6). Four candidates from each library (Z_{VEGFR2_11}, Z_{VEGFR2_16}, Z_{VEGFR2_19} and Z_{VEGFR2_22} from $Z_{VEGFR2\_1matlib}$, and Z_{VEGFR2_33}, Z_{VEGFR2_38}, Z_{VEGFR2_40} and Z_{VEGFR2_41} from $Z_{VEGFR2\_2matlib}$) were produced as His_6-tagged soluble proteins for further downstream characterizations.

Analysis of secondary structure content, thermal stability and refolding capacity. Secondary structure content of the eight selected candidates was analyzed by CD spectroscopy, in principle

Table 1 | Library design of affinity maturation library $Z_{VEGFR2\_1matlib}$

	Positions												
Codons	9	10	11	13	14	17	18	24	25	27	28	32	35
AAA (Lys)	0.6	0.9	47.8	1.2	3.9	0.3	1.1	0.4	21.7	0.3	0.5	0.3	0.4
AAC (Asn)	89.7	0.9	3.1	1.2	33.4	0.3	81.8	0.4	4.6	0.3	0.5	0.3	0.4
ACT (Thr)	0.6	0.9	3.1	1.2	3.9	0.3	1.1	0.4	4.6	0.3	0.5	0.3	0.4
ATC (Ile)	0.6	0.9	3.1	1.2	3.9	0.3	1.1	0.4	4.6	0.3	90.8	0.3	0.4
ATG (Met)	0.6	0.9	3.1	1.2	3.9	0.3	1.1	0.4	4.6	0.3	0.5	0.3	0.4
CAG (Gln)	0.6	0.9	3.1	1.2	3.9	0.3	1.1	0.4	4.6	0.3	0.5	0.3	0.4
CAT (His)	0.6	0.9	3.1	1.2	3.9	0.3	1.1	0.4	4.6	0.3	0.5	0.3	0.4
CCG (Pro)	0	0	0	0	0	0	0	0	0	0	0	0	0
CGT (Arg)	0.6	0.9	3.1	1.2	3.9	0.3	1.1	0.4	4.6	0.3	0.5	0.3	0.4
CTG (Leu)	0.6	85.4	3.1	1.2	3.9	0.3	1.1	0.4	4.6	0.3	0.5	0.3	92.5
GAA (Glu)	0.6	0.9	3.1	1.2	3.9	0.3	1.1	0.4	4.6	0.3	0.5	0.3	0.4
GAC (Asp)	0.6	0.9	3.1	1.2	3.9	0.3	1.1	93.3	4.6	0.3	0.5	0.3	0.4
GCT (Ala)	0.6	0.9	3.1	1.2	3.9	94.2	1.1	0.4	4.6	0.3	0.5	0.3	0.4
GGT (Gly)	0.6	0.9	3.1	1.2	3.9	0.3	1.1	0.4	4.6	0.3	0.5	0.3	0.4
GTT (Val)	0.6	0.9	3.1	1.2	3.9	0.3	1.1	0.4	4.6	0.3	0.5	0.3	0.4
TAC (Tyr)	0.6	0.9	3.1	1.2	3.9	0.3	1.1	0.4	4.6	94.8	0.5	95.1	0.4
TCT (Ser)	0.6	0.9	3.1	80.3	3.9	0.3	1.1	0.4	4.6	0.3	0.5	0.3	0.4
TGC (Cys)	0	0	0	0	0	0	0	0	0	0	0	0	0
TGG (Trp)	0.6	0.9	3.1	1.2	3.9	0.3	1.1	0.4	4.6	0.3	0.5	0.3	0.4
TTC (Phe)	0.6	0.9	3.1	1.2	3.9	0.3	1.2	0.4	4.6	0.3	0.5	0.3	0.4

The percentages of the codons used in each of the thirteen randomized library positions are indicated.

Table 2 | Library design of affinity maturation library $Z_{VEGFR2\_2matlib}$

	Positions												
Codons	9	10	11	13	14	17	18	24	25	27	28	32	35
AAA (Lys)	1	1.7	2.2	0.9	2.3	1	1.6	1.1	1.7	0.8	0.8	0.8	1.1
AAC (Asn)	1	1.7	2.2	0.9	2.3	1	1.6	1.1	1.7	0.8	0.8	0.8	1.1
ACT (Thr)	1	1.7	2.2	0.9	2.3	1	1.6	1.1	1.7	0.8	0.8	0.8	1.1
ATC (Ile)	1	1.7	2.2	0.9	2.3	1	1.6	1.1	1.7	0.8	0.8	0.8	1.1
ATG (Met)	1	1.7	2.2	0.9	2.3	1	1.6	1.1	1.7	0.8	0.8	0.8	1.1
CAG (Gln)	1	70.3	2.2	0.9	2.3	1	1.6	1.1	1.7	0.8	0.8	0.8	1.1
CAT (His)	1	1.7	2.2	0.9	2.3	1	1.6	81.1	1.7	0.8	0.8	0.8	1.1
CCG (Pro)	0	0	0	0	0	0	0	0	0	0	0	0	0
CGT (Arg)	1	1.7	2.2	0.9	61.2	83.5	1.6	1.1	1.7	0.8	0.8	0.8	1.1
CTG (Leu)	1	1.7	2.2	0.9	2.3	1	1.6	1.1	1.7	0.8	0.8	0.8	1.1
GAA (Glu)	1	1.7	2.2	0.9	2.3	1	1.6	1.1	1.7	0.8	0.8	0.8	1.1
GAC (Asp)	1	1.7	2.2	84.2	2.3	1	1.6	1.1	1.7	0.8	0.8	0.8	1.1
GCT (Ala)	1	1.7	2.2	0.9	2.3	1	72.6	1.1	1.7	0.8	0.8	0.8	1.1
GGT (Gly)	1	1.7	2.2	0.9	2.3	1	1.6	1.1	71.1	0.8	0.8	0.8	1.1
GTT (Val)	1	1.7	2.2	0.9	2.3	1	1.6	1.1	1.7	0.8	0.8	86.9	1.1
TAC (Tyr)	1	1.7	2.2	0.9	2.3	1	1.6	1.1	1.7	0.8	86.2	0.8	81.1
TCT (Ser)	1	1.7	61.8	0.9	2.3	1	1.6	1.1	1.7	0.8	0.8	0.8	1.1
TGC (Cys)	0	0	0	0	0	0	0	0	0	0	0	0	0
TGG (Trp)	1	1.7	2.2	0.9	2.3	1	1.6	1.1	1.7	86.5	0.8	0.8	1.1
TTC (Phe)	82.4	1.7	2.2	0.9	2.3	1	1.6	1.1	1.7	0.8	0.8	0.8	1.1

The percentages of the codons used in each of the thirteen randomized library positions are indicated.

as described above (Supplementary Fig. S7). All clones showed an alpha-helical content, although Z_{VEGFR2_11} had a relatively lower degree of alpha-helicity. All candidates demonstrated a similar secondary structure content as for non-heat treated samples when lowering the temperature back to 20°C after heating to 91°C, indicating efficient refolding (Supplementary Fig. S7). The melting temperatures of the clones obtained from $Z_{VEGFR2\_1matlib}$ were around 45°C (Table 3). Notably, the three clones from the $Z_{VEGFR2\_2matlib}$ containing the K33N mutation (Z_{VEGFR2_41}, Z_{VEGFR2_38}, Z_{VEGFR2_33}) showed a lower melting temperature than both the first generation binder Z_{VEGFR2_2} and the second generation binder Z_{VEGFR2_40}, lacking the K33N mutation (Table 3; Supplementary Table S1; Supplementary Fig. S7), indicating that the non-intended mutation in position 33 had a negative influence on the thermal stability. Z_{VEGFR2_41}, Z_{VEGFR2_38} and Z_{VEGFR2_33} were therefore excluded from further characterizations. Z_{VEGFR2_11} was also excluded, due to the relatively lower degree of alpha-helical structure content.

Affinity determination of second-generation binders. Binding kinetics of Z_{VEGFR2_22}, Z_{VEGFR2_19}, Z_{VEGFR2_16} and Z_{VEGFR2_40} were analyzed using surface plasmon resonance (Fig. 4a; Supplementary Fig. S8). Data was fitted using non-linear regression to a monovalent binding model and the equilibrium dissociation constants (K_D) were calculated from the obtained association and dissociation rate constants. Equilibrium dissociation constants for human VEGFR2 were determined to 5.0 nM–10.9 nM for the four candidates (Table 3), representing around a 30-fold and a 7-fold increase in affinity compared to the original binders Z_{VEGFR2_1} and Z_{VEGFR2_2}, respectively. The affinities for murine VEGFR2 were determined to 7.8 nM–11.9 nM, representing around a 30-fold and an 8-fold increase in affinity compared to first-generation binders (Table 3). The affinity-matured variants Z_{VEGFR2_22} and Z_{VEGFR2_40} were selected for further studies.

SPR-based competition assays. In order to confirm that the affinity-matured variants had retained the ability to bind simultaneously to VEGFR2 and compete with VEGF-A, two SPR-based competition assays were conducted. In the first assay, human VEGFR2 was immobilized on the sensor chip. Analysis of potential simultaneous binding of Z_{VEGFR2_22} and Z_{VEGFR2_40} to the receptor was performed using a double injection, as described above. As for the previous experiments, injection of the mix resulted in a substantially higher signal, confirming that the affinity-matured candidates had retained the ability to bind simultaneously to VEGFR2 (Fig. 4b; Supplementary Fig. S9).

The second competition assay was performed to verify that the affinity-matured Affibody molecules could block VEGF-A from binding to VEGFR2. Human or murine VEGF-A was immobilized on the chip surface. VEGFR2 was preincubated with Z_{VEGFR2_22}, Z_{VEGFR2_40} or PBS, followed by injection over the surface. Injection of the control sample, containing VEGFR2 pre-incubated with PBS, resulted in an increase in signal, showing binding of VEGFR2 to VEGF. In contrast, injection of the samples containing VEGFR2 preincubated with the Affibody molecules resulted in a substantially lower response, showing that the Affibody molecules blocked the interaction between VEGFR2 and VEGF-A (Fig. 4c; Supplementary Fig. S10). The results from the competition assays hence demonstrated that the affinity-matured Affibody molecules retained both the ability to simultaneously interact with VEGFR2, and block human as well as murine VEGF-A from binding to the receptor.

Design and production of dimeric VEGFR2-binding Affibody molecules. Next, we investigated whether engineering of bi-paratopic constructs, comprising the two different VEGFR2-specific Affibody molecules, might result in a further increase in VEGFR2 affinity due to potential avidity effects as well as an increase in VEGFR2-binding surface area. Two heterodimeric fusion proteins in different orientations were designed: i) Z_{VEGFR2_22}-$(S_4G)_4$-ABD_{035}-$(S_4G)_4$-Z_{VEGFR2_40} and ii) Z_{VEGFR2_40}-$(S_4G)_4$-ABD_{035}-$(S_4G)_4$-Z_{VEGFR2_22} (Fig. 5a). Moreover, two homodimeric constructs (Z_{VEGFR2_22}-$(S_4G)_4$-ABD_{035}-$(S_4G)_4$-Z_{VEGFR2_22} and Z_{VEGFR2_40}-$(S_4G)_4$-ABD_{035}-$(S_4G)_4$-Z_{VEGFR2_40}) were included as controls (Fig. 5a). Serine/glycine-based linkers (20 aa) were included between the three domains to increase the possibility for simultaneous binding to both epitopes. The

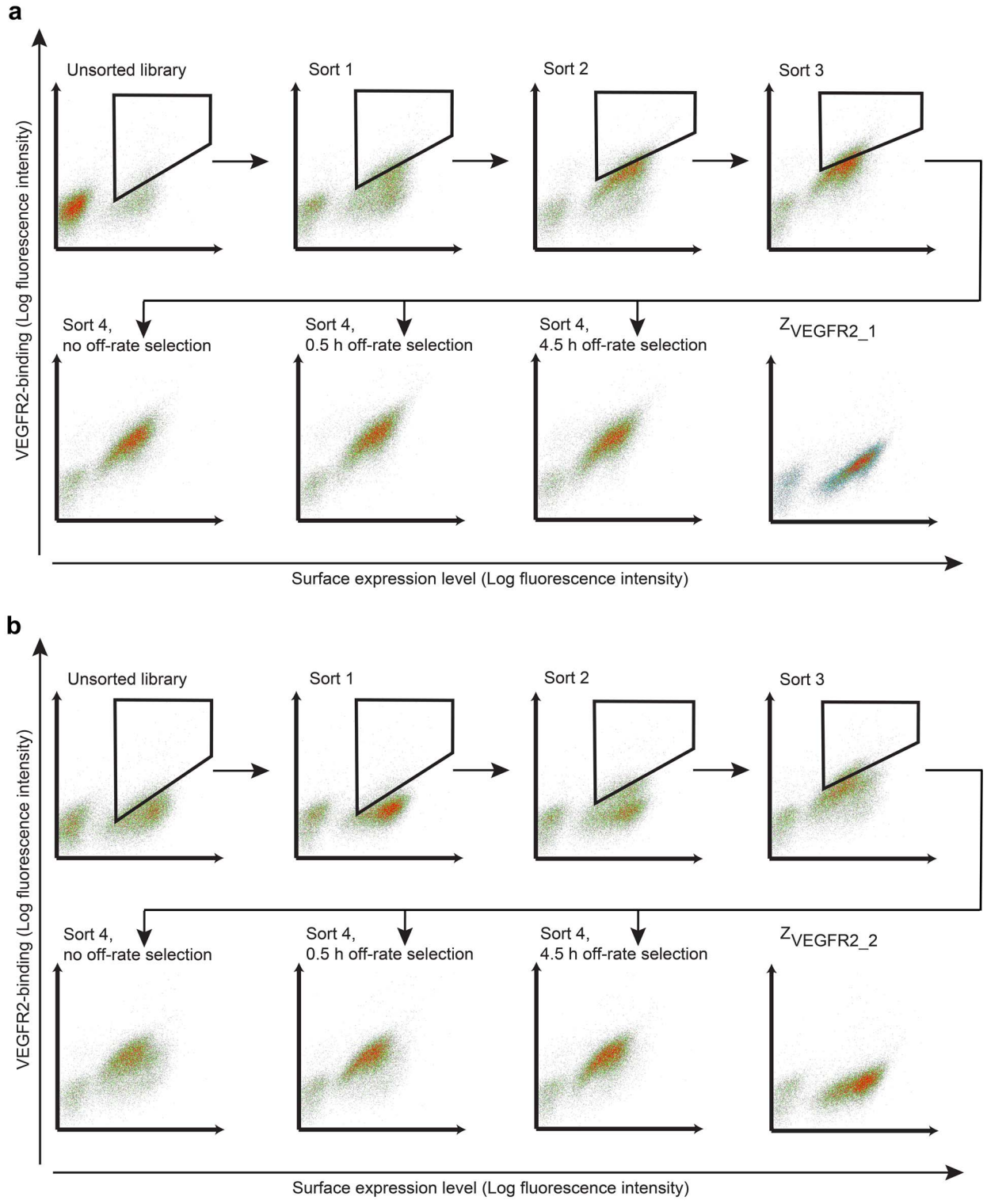

Figure 3 | Sorting of the affinity maturation libraries. (a) $Z_{VEGFR2\_1matlib}$ (b) $Z_{VEGFR2\_2matlib}$ displayed on staphylococcal cells. The VEGFR2 binding signal (monitored by the binding of fluorescently labeled anti-Fc antibody to human VEGFR2/Fc) is represented on the Y axis and the surface expression level (monitored by fluorescently labeled HSA binding) is represented on the X axis. The dot plots show staphylococcal cell populations from the original unsorted library as well as cell populations isolated in the 1st, 2nd, 3rd and 4th selection round, respectively. For the 4th selection round, dot plots are shown for selections including an off-rate experiment of 0 min, 30 min or 4.5 h.

albumin-binding domain (ABD_{035}) domain has previously been engineered to femtomolar affinity for HSA[32], and was intended to serve a potential means for future in vivo half-life extension[33,34]. In addition, ABD would function as an additional linker, as well as a detection tag or as a purification tag for convenient recovery by affinity chromatography. The four constructs were expressed in *E. coli* and purified by affinity chromatography using HSA-sepharose. SDS-PAGE and MALDI-time of flight (TOF) mass spectrometry confirmed that the proteins were pure and had the correct molecular weights (data not shown).

Table 3 | Equilibrium dissociation constants (K_D), dissociation rate constants (k_d) and estimated melting temperatures (Tm) for affinity-matured Affibody molecules

Denotation	Average K_D (nM) for murine VEGFR2 (±SD)	Average K_D (nM) for human VEGFR2 (±SD)	Average k_d (s^{-1}) for human VEGFR2 (±SD)	Average k_d (s^{-1}) for murine VEGFR2 (±SD)	Estimated Tm (°C)
Z_{VEGFR2_22}	9.8 ± 3.5	5.0 ± 0.2	$5.8 \times 10^{-3} \pm 4.2 \times 10^{-4}$	$8.6 \times 10^{-3} \pm 4.0 \times 10^{-4}$	49
Z_{VEGFR2_19}	10.0 ± 2.4	5.4 ± 0.8	$4.2 \times 10^{-3} \pm 6.3 \times 10^{-4}$	$1.1 \times 10^{-2} \pm 1.5 \times 10^{-4}$	47
Z_{VEGFR2_11}	ND	ND	ND	ND	47
Z_{VEGFR2_16}	11.9 ± 3.9	6.7 ± 1.1	$5.6 \times 10^{-3} \pm 3.1 \times 10^{-4}$	$1.2 \times 10^{-2} \pm 5.5 \times 10^{-4}$	46
Z_{VEGFR2_41}	ND	ND	ND	ND	34
Z_{VEGFR2_38}	ND	ND	ND	ND	34
Z_{VEGFR2_33}	ND	ND	ND	ND	39
Z_{VEGFR2_40}	7.8 ± 3.4	10.9 ± 3.1	$1.5 \times 10^{-2} \pm 1.5 \times 10^{-3}$	$1.1 \times 10^{-2} \pm 1.9 \times 10^{-3}$	45

SPR-based analysis of dimeric constructs. The binding of the four dimeric constructs to human and murine VEGFR2 was analyzed in a biosensor assay. We needed to immobilize the dimeric Affibody molecules on the chip surface and inject soluble monomeric VEGFR2 in order to be able to reveal any potential avidity effects. Moreover, we also wanted to assess whether the new constructs could interact with the receptor while simultaneously binding to albumin, which would be essential for future in vivo experiments. HSA was therefore covalently immobilized on the chip and the dimeric constructs were injected over respective surfaces, resulting in a directed non-covalent immobilization of the Affibody constructs on the chip (Fig. 5a). The dissociation of the Affibody constructs from the surface was practically negligible, due to the femtomolar affinity of ABD_{035} for HSA[32]. Monomeric human VEGFR2 was thereafter injected over the surfaces (Fig. 5b). The complex mode of interaction resulted in difficulties to fit the association phase to a 1 : 1 binding model and assessment was focused on the dissociation phase. It should be noted that any avidity effects due to simultaneous binding for the heterodimers were expected to mainly influence the off-rate and potential improvements in dissociation should hence reflect improvements in equilibrium binding. The heterodimeric constructs demonstrated a substantially slower dissociation compared to the homodimeric controls (Fig. 5c; Supplementary Fig. S11). For the best-performing of the heterodimeric constructs (Z_{VEGFR2_22}-$(S_4G)_4$-ABD_{035}-$(S_4G)_4$-Z_{VEGFR2_40}), the dissociation rate constant was estimated to around 8.4×10^{-5} s^{-1} for human VEGFR2. The respective dissociation rate constants for the monomeric Z_{VEGFR2_22} and Z_{VEGFR2_40} were around 5.8×10^{-3} s^{-1} and 1.5×10^{-2} s^{-1} (Table 3). The improvements achieved by formatting the Affibody molecules as biparatopic binders corresponded to around 70-fold and 180-fold slower off-rate, respectively. In comparison to the respective homodimeric constructs, the improvement in dissociation rate constants corresponded to around a 14-fold and a 20-fold. Dissociation rate constants for the dimeric Affibody constructs are summarized in Table 4. The slower dissociation rates for the heterodimeric constructs verified that Z_{VEGFR2_22} and Z_{VEGFR2_40} could bind simultaneously to VEGFR2 also when linked together in one fusion protein. Consequently, the assay showed that the two epitopes are non-overlapping and located in relatively close proximity on the receptor. The results also revealed that the multimeric binders could target VEGFR2 and at the same time bind to HSA, which thus demonstrated that including ABD in the biparatopic constructs is a promising means for prolonging the circulatory half-life in vivo.

Flow-cytometric analysis of mammalian cell binding. In order to verify that the dimeric Affibody constructs could bind to VEGFR2 expressed on the surface of mammalian cells, a flow-cytometry based assay was performed. HEK 293 cells transfected with human VEGFR2 (293/KDR cells) (Sibtech Inc.), were incubated with the four dimeric construct. To assess whether the Affibody constructs could target the mammalian cells while simultaneously being bound to albumin, fluorescently labeled HSA was used as a secondary reagent. An Affibody construct with non-relevant specificity (Z_{Taq}-$(S_4G)_4$-ABD_{035}-$(S_4G)_4$-Z_{Taq}, specific for Taq polymerase) was included as negative control. In addition, non-transfected HEK293 cells were included as controls in the assay to verify that potential cell binding was specific for VEGFR2. An anti-human VEGFR2 monoclonal antibody (R&D Systems) was included as a positive control. A shift in fluorescence intensity was observed for the 293/KDR cells incubated with all the VEGFR2-specific Affibody constructs compared to the negative control construct or cells labeled with only secondary reagent (Fig. 5d). Moreover, the samples with non-transfected HEK293 cells were negative in the assay, suggesting that the Affibody molecules specifically targeted VEGFR2 on the surface of the mammalian cells (Supplementary Fig. S12). The positive control antibody confirmed that VEGFR2 was present at the cell surface of 293/KDR but not on HEK293 cells (Supplementary Fig. S12). Incubation with heterodimeric constructs resulted in higher fluorescence signal intensity compared to the homodimeric constructs, confirming that the heterodimeric constructs had higher affinities for VEGFR2 also expressed on the cell surface.

Inhibition of VEGF-A induced phosphorylation of VEGFR2. In order to investigate if the VEGFR2-specific Affibody molecules could inhibit VEGFR2 phosphorylation, an ELISA-based phosphorylation assay was performed. 293/KDR cells were incubated with 3 nM or 30 nM of the biparatopic binder Z_{VEGFR2_22}-$(S_4G)_4$-ABD_{035}-$(S_4G)_4$-Z_{VEGFR2_40}, a combination of 30 nM or 3 nM of each of Z_{VEGFR2_22} and Z_{VEGFR2_40}, 30 nM or 3 nM of the negative control construct Z_{Taq}-$(S_4G)_4$-ABD_{035}-$(S_4G)_4$-Z_{Taq}, or PBS only. After incubation with the Affibody molecules, VEGFR2 phosphorylation was stimulated by incubation with human VEGF-A. Cells were lysed and the degree of phosphorylation on VEGFR2 Tyr1175 was analyzed by ELISA.

The results revealed a decrease in signal for cells that were treated with VEGFR2-specific Affibody molecules, demonstrating inhibition of VEGFR2 signaling (Fig. 5e). The biparatopic binder resulted in a more potent inhibition of phosphorylation than the combination of the two monomeric binders.

Discussion

Activation of angiogenesis is a critical step in tumor development and other diseases[3,4]. With the aim to target angiogenesis, we generated biparatopic VEGFR2-specific Affibody molecules, with high affinities for human as well as murine VEGFR2. Phage display was used for the selection of two Affibody molecules, which were cross-reactive to human as well as murine VEGFR2. The cross-reactivity to murine VEGFR2 is valuable for preclinical studies in mouse models. Due to the complex regulatory role of VEGFR1 in angiogenesis[35], cross-reactivity to this receptor might complicate future *in vivo* studies. Cross-reactivity to VEGFR3 should preferably also be avoided

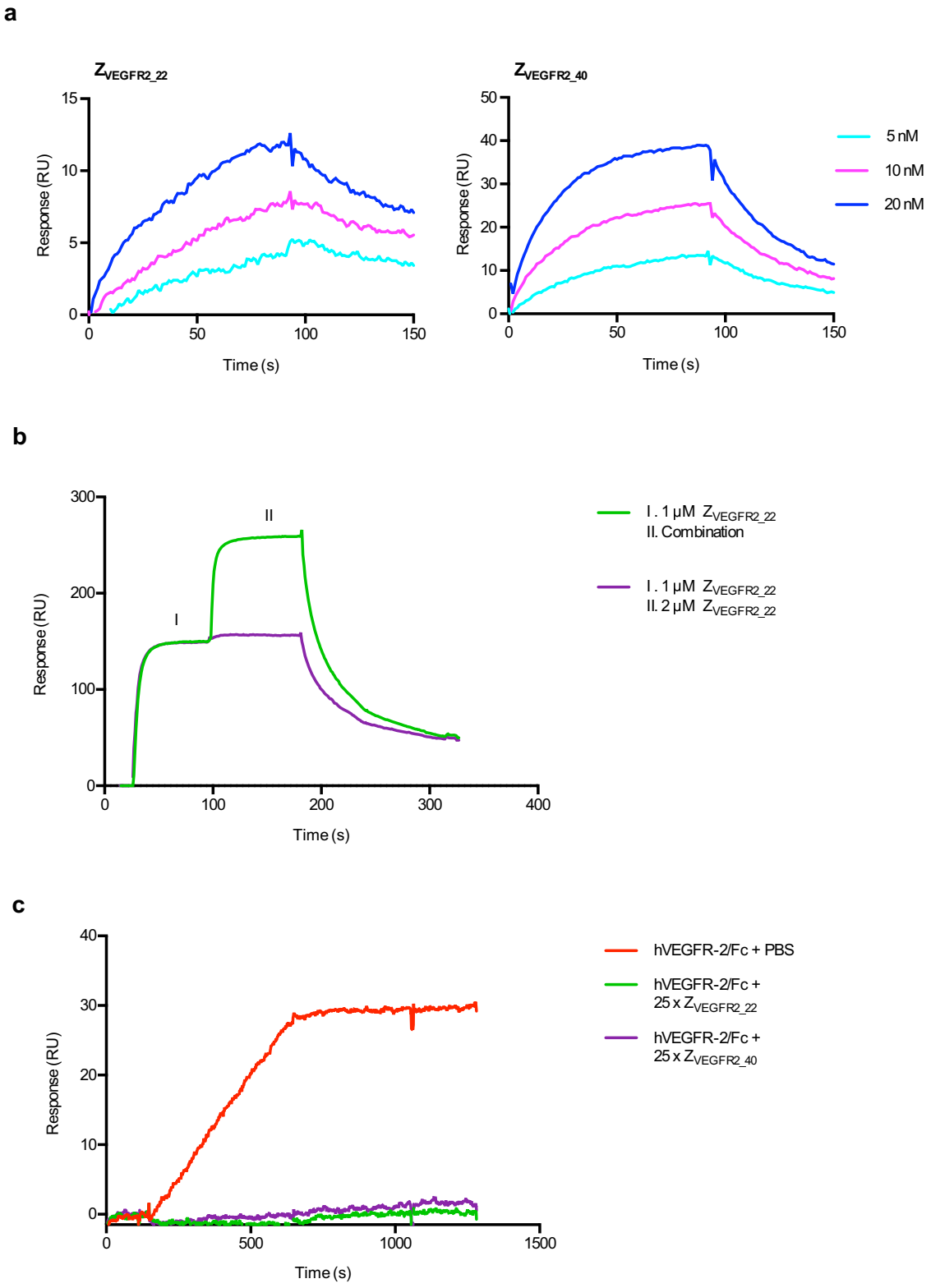

Figure 4 | Characterization of affinity matured VEGFR2-binding Affibody molecules selected by staphylococcal display. (a) Representative sensorgrams from SPR analysis of affinity-matured Affibody molecules (Z_{VEGFR2_22} and Z_{VEGFR2_40}) binding to immobilized VEGFR2, showing the response signal. Affibody molecules were injected at concentrations of 5, 10 and 20 nM. Data is referenced by subtraction of simultaneous responses from reference surface. The experiment was performed in duplicates. (b) Representative results from SPR-based competition assay. Sensorgrams were obtained from a double injection, where 1 µM of Z_{VEGFR2_22} was injected (1), immediately followed by a second injection (2) of either a combination of 1 µM of Z_{VEGFR2_22} and 1 µM of Z_{VEGFR2_40}, or 2 µM of Z_{VEGFR2_22}, over immobilized human or murine VEGFR2. The experiment was performed in duplicates. (c) Representative results from SPR-based assay of VEGF blocking. 40 nM of human VEGFR2, which had been pre-incubated for 40 min with a 25 × molar excess of Z_{VEGFR2_22}, was injected over a surface of immobilized human VEGF-A. The experiment was performed in duplicates.

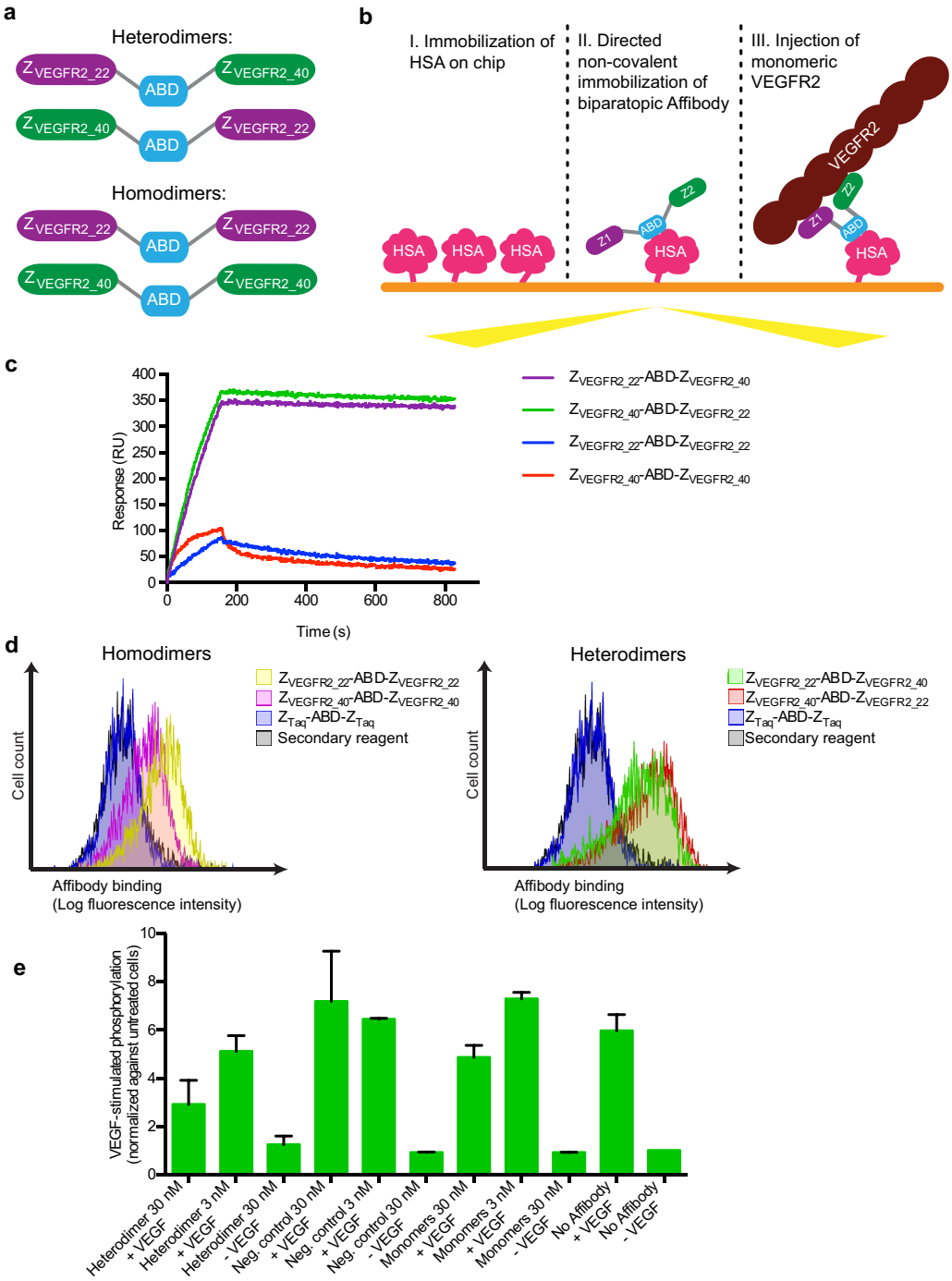

Figure 5 | Characterization of biparatopic Affibody constructs. (a) Schematic overview of the design of the dimeric constructs. (b) Schematic overview of SPR-based off rate analysis assay. HSA was immobilized on the chip surface. A first injection of dimeric Affibody constructs resulted in a negligible off rate due to the femtomolar affinity of ABD for HSA. VEGFR2 binding was analyzed by subsequent injection of monomeric VEGFR2. The experiments were performed in duplicates. (c) Representative sensorgrams obtained from the SPR-based off-rate analysis assay, showing the injection of 40 nM monomeric human VEGFR2 over each of the four dimeric Affibody molecules. Data is double referenced by subtraction of simultaneous responses from reference surface and a buffer injection. (d) Flow-cytometric analysis of binding of dimeric Affibody constructs to VEGFR2-expressing 293/KDR cells. Binding of the Affibody constructs is monitored by the binding of fluorescently labeled HSA to the ABD tag. A higher shift in mean log fluorescence intensity compared to the negative control construct Z_{Taq}-ABD-Z_{Taq} or cells labeled with secondary reagent only was observed for the heterodimeric constructs than for the homodimeric constructs upon binding to VEGFR2-expressing cells. The experiment was performed in duplicates. (e) Inhibition of VEGF-A induced phosphorylation of VEGFR2 on 293/KDR cells. Cells were pre-treated with the biparatopic binder Z_{VEGFR2_22}-$(S_4G)_4$-ABD_{035}-$(S_4G)_4$-Z_{VEGFR2_40}, a combination of 30 nM or 3 nM of each of the monomeric binders Z_{VEGFR2_22} and Z_{VEGFR2_40}, 30 nM or 3 nM of the negative control construct Z_{Taq}-ABD_{035}-Z_{Taq}, or PBS, followed by stimulation with VEGF-A. VEGFR2 phosphorylation was determined by ELISA. The biparatopic binder and the combination of monomers both resulted in a decrease in phosphorylation level compared to the controls, and a more potent inhibition was observed for the biparatopic binder. The data is presented as the OD450 for each sample normalized against the OD450 of untreated cells. The experiment was performed in duplicates.

Table 4 | Dissociation rate constants (k_d) for dimeric Affibody constructs

Construct	Average k_d (s^{-1}) for human VEGFR2 (±SD)	Average k_d (s^{-1}) for murine VEGFR2 (±SD)
Z_{VEGFR2_22}-ABD-Z_{VEGFR2_40}	$8.4 \times 10^{-5} \pm 3.5 \times 10^{-5}$	$1.4 \times 10^{-4} \pm 1.8 \times 10^{-5}$
Z_{VEGFR2_40}-ABD-Z_{VEGFR2_22}	$1.5 \times 10^{-4} \pm 4.2 \times 10^{-5}$	$1.8 \times 10^{-4} \pm 2.2 \times 10^{-5}$
Z_{VEGFR2_22}-ABD-Z_{VEGFR2_22}	$1.6 \times 10^{-3} \pm 8.7 \times 10^{-5}$	$9.9 \times 10^{-4} \pm 2.0 \times 10^{-4}$
Z_{VEGFR2_40}-ABD-Z_{VEGFR2_40}	$1.2 \times 10^{-3} \pm 1.5 \times 10^{-4}$	$7.9 \times 10^{-4} \pm 4.9 \times 10^{-4}$

due to potential unwanted effects on lymphatic vessels[35]. Results from the ELISA-based specificity experiments demonstrated that the two variants did not cross-react with VEGFR1 or VEGFR3. The results also indicated that the Affibody molecules recognized the same or partially overlapping epitopes on VEGFR2 as the natural ligand VEGF-A, which is promising for future therapeutic approaches with the aim to block the interaction between VEGF and the receptor.

To improve the two candidates even further, we initiated an affinity maturation effort. Staphylococcal surface display has previously been successful for generating high-affinity Affibody molecules from affinity maturation libraries[31,36]. An advantage of cell surface display is the possibility to sort libraries using flow cytometry, which enables real-time monitoring of the selection process and efficient affinity discrimination using fine-tuned sort gates. Isolation of second-generation candidates by FACS was successful and the best variants had an affinity in the single-digit nanomolar range.

SPR experiments indicated that the two Affibody molecules bind to different epitopes on VEGFR2. Both binders also competed with VEGF, suggesting that the two different binding sites might be situated relatively close to each other. Based on these results, we reasoned that a possible strategy for obtaining an additional increase in affinity would be to engineer so-called biparatopic Affibody constructs, i.e. dimers with two different paratopes, recognizing two distinct sites on VEGFR2. We also included a high-affinity albumin-binding domain to get a first indication whether ABD-fusions might be a promising strategy for prolonging circulation time of the biparatopic Affibody molecules in future in vivo experiments. The biparatopic format was successful and connecting the two Affibody molecules with flexible linkers resulted in dramatically slower dissociation kinetics. Although the association rate constants were difficult to determine, the off-rate was in the same range as for the high-affinity HER2-specific Affibody molecule (K_D of 22 pM)[22]. Interestingly, the off-rate was also similar as for the full-length bivalent IMC-1121B (Ramucirumab)[16], suggesting a comparable affinity as the much larger antibody. Data also revealed that the format allowed for simultaneous interaction with VEGFR2 and albumin, both in biosensor assays on recombinant receptor as well as in flow-cytometry experiments with VEGFR2-positive mammalian cells. Furthermore, one of the biparatopic binders was tested for the ability to inhibit VEGF-A induced phosphorylation of VEGFR2 expressed on mammalian cells. A substantial decrease in phosphorylation level was observed after treatment with the biparatopic binder, suggesting that this Affibody construct had an antagonistic effect on VEGFR2 signaling, which is promising for future therapeutic applications. The results also demonstrated a more potent inhibition by the biparatopic binder than a combination of each of the monomeric binders, confirming the higher affinity of the heterodimeric format.

Although the trivalent Affibody molecules with ABD comprised three domains and two linkers, the size was still relatively small (around 22 kDa), which is smaller than an scFv. The small size of the Affibody makes it potentially well-suited for applications where an alternative route of administration (e.g. eye drops) is necessary or beneficial. This could be an important advantage compared to larger molecules, such as antibodies, for treatment of neovascular eye conditions[37].

In future studies, additional optimizations of for example orientation of the domains, linker length and linker composition might improve the properties even further. Competition with VEGF-A suggests that the Affibody molecules also recognize domain 2 and/or domain 3 on the extracellular part of VEGFR2. Mapping the epitopes in fine detail would likely result in valuable insights regarding the modes of binding and potential new strategies for further protein engineering. Moreover, as mentioned above, Affibody molecules are excellent for construction of various bi- and multispecific variants, and combining the biparatopic VEGFR2-binder with Affibody molecules for other targets or payloads might allow for design of even more potent agents. Recently, several studies have reported on arming monoclonal antibodies with various Affibody molecules to efficiently achieve bi- or even multispecific mAbs (so-called AffiMabs[38,39]. Such AffiMabs retain the properties of the original antibody, but with an additional specificity mediated by the Affibody molecules. We believe that our new Affibody molecules would be excellent for adding VEGFR2-specificity to already existing mAbs or other affinity proteins, a strategy that has previously been demonstrated to generate promising results[40–42]. Finally, this is the first report on the engineering of biparatopic Affibody molecules, and the successful results showed that it is an efficient approach for increasing the affinity and it might become a general future strategy for improving the potency of various Affibody molecules.

Methods

Selection of Affibody molecules using phage display. A combinatorial library of Affibody molecule variants displayed on bacteriophage was subjected to four rounds of selection using human VEGFR2/Fc (hVEGFR2/Fc, R&D Systems, Minneapolis, MN, USA), essentially as described by Grönwall *et al*[43]. Selection was followed by ELISA screening for analysis of VEGFR2-binding, specificity and VEGF-A blocking. Details are provided in Supplementary methods and Supplementary Table S1 online.

Subcloning, protein production and purification of Z_{VEGFR2_1} and Z_{VEGFR2_2}. Subcloning of the genes encoding Z_{VEGFR2_1} and Z_{VEGFR2_2} into the pET-26b(+) vector followed by soluble protein production and purification was performed as previously described[21], and the buffer was exchanged to PBS using PD-10 columns (GE Healthcare, Uppsala, Sweden).

Circular dichroism analysis of Z_{VEGFR2_1} and Z_{VEGFR2_2}. The purified proteins were analyzed by circular dichroism (CD) spectroscopy as previously described[21].

Binding kinetics analysis of Z_{VEGFR2_1} and Z_{VEGFR2_2}. Surface plasmon resonance (SPR) experiments were performed using a ProteOn XPR36 instrument (Biorad Laboratories, Hercules, CA, USA) using phosphate-buffered saline supplemented with 0.1% Tween 20 (PBST 0.1) as running buffer and 10 mM HCl or PBST 0.1 for regeneration. Human and murine VEGFR2/Fc (R&D systems) were immobilized by amine coupling on two surfaces of a GLM sensor chip (Biorad Laboratories). Binding of Z_{VEGFR2_1} and Z_{VEGFR2_2} to both human and murine VEGFR2 was analyzed by injections of five different concentrations of the Affibody molecules (50, 100, 200, 350 and 500 nM) over the immobilized VEGFR2/Fc. PBST 0.1 was used as a running buffer and 10 mM HCl for regeneration. The experiment was performed in duplicates using freshly prepared reagents.

Surface plasmon resonance-based competition assays. Competition assays were performed using a BIAcore™ 3000 instrument (GE Healthcare). All experiments were performed in duplicates using freshly prepared reagents, with PBST 0.1 as a running buffer and 10 mM NaOH for regeneration. For analysis of potential simultaneous binding of Z_{VEGFR2_1} and Z_{VEGFR2_2} to VEGFR2, human and murine VEGFR2/Fc (R&D Systems) was immobilized on a CM-5 sensor chip (GE Healthcare). First, 1 μM of Z_{VEGFR2_1} was injected, directly followed by an injection of a mixture of 1 μM Z_{VEGFR2_1} and 1 μM Z_{VEGFR2_2}, or 2 μM Z_{VEGFR2_1} as a control. In a second assay, Z_{VEGFR2_2} was injected first, followed by a mixture of Z_{VEGFR2_1} and Z_{VEGFR2_2}, or 2 μM Z_{VEGFR2_2}.

For analysis of competition with VEGF-A, human or murine VEGF-A (R&D Systems) was immobilized on a sensor chip surface. 40 nM of human or murine VEGFR2/Fc (R&D Systems), which had been preincubated with a 25-fold molar excess of Z_{VEGFR2_1} or Z_{VEGFR2_2} (or PBS, as a control) for 40 min, was injected over the surface.

Construction of single-point mutations for alanine scan of Z_{VEGFR2_1} and Z_{VEGFR2_2}. Single-point mutations of Z_{VEGFR2_1} and Z_{VEGFR2_2} with substitution to codon for alanine in residues 9, 10, 11, 13, 14, 17 (not in Z_{VEGFR2_1}), 18 (not in Z_{VEGFR2_2}), 24, 25, 27, 32 or 35 were constructed by PCR amplification using oligonucleotides encoding for each mutation. Residues Ala17 in Z_{VEGFR2_1} and Ala18 in Z_{VEGFR2_2} were mutated to valine. Cloning of the mutant sequences into the staphylococcal display vector pSCZ1 and transformation to *S. carnosus* was performed essentially as previously described[21], but using restriction enzymes *Xho*I and *Sac*I.

Flow-cytometric analysis of alanine scan mutants. Flow-cytometric analysis of each alanine (or valine) mutant was performed essentially as previously described[21], using 100 nM human or murine VEGFR2/Fc (R&D Systems). Details are provided in Supplemetary methods online.

Construction of affinity maturation libraries. Two affinity maturation libraries were designed and randomized oligonucleotides encoding helix 1 and 2 of the Affibody molecules were purchased from Isogenica (Isogenica, Essex, UK). The libraries were amplified by 15 cycles of PCR using Phusion DNA polymerase (Finnzymes), and the PCR products were purified using QIAquick PCR purification kit (Qiagen) and digested with restriction enzymes *Xho*I and *Sac*I, followed by purification using preparative gel electrophoresis (2% agarose gel) and a QIAquick gel extraction kit (Qiagen). The staphylococcal display vector pSCZ1 was digested with the same restriction enzymes and purified by preparative gel electrophoresis as described above. The libraries were ligated into pSCZ1 using T4 DNA ligase (New England Biolabs), according to the supplier's recommendations. Plasmids were purified and concentrated using phenol chloroform extraction and ethanol precipitation, and subsequently transformed to *E. coli* SS320 (MC1061 F′) electrocompetent cells (Lucigen, Middleton, WI, USA). Plasmids were prepared and transformed to *S. carnosus* by electroporation as previously described[44]. 192 colonies were analyzed by sequencing.

FACS from bacteria-displayed Affibody libraries. Aliquots of the libraries containing 1.2×10^9 cells (30-fold the estimated library size) were inoculated to 500 ml TSB + YE (Merck) with 10 μg/ml chloramphenicol (Sigma-Aldrich), and incubated at 150 rpm and 37°C for 24 h. Around 10^9 cells were harvested by centrifugation and labelled for flow cytometry essentially as described above for the alanine scan mutants, using 1.5 ml of 20 nM hVEGFR2/Fc (R&D Systems) in a first incubation of 2 h, and 800 μl of the secondary Antibody and HSA in a second incubation of 45 min. Before sorting, cells were washed three times in ice-cold PBSP and re-suspended in 1.4 ml ice-cold PBSP. Four rounds of sorting of the libraries were performed using a MoFlo Astrios flow cytometer (Beckman Coulter, Indianapolis, IN, USA). In sorting round 2–4, approximately 10 × the library size was labeled for sorting. Around 0.5% of the population, with the highest VEGFR2-binding signal, was gated and sorted to TSB + YE (Merck), and grown overnight with 10 μg/ml chloramphenicol (Sigma-Aldrich). In the first round, the libraries were incubated with 50 nM hVEGFR2/Fc, and in the second and third round with 5 nM hVEGFR2/Fc. In the fourth round, an off-rate selection strategy was applied. First, cells were incubated with 20 nM hVEGFR2/Fc (R&D Systems) as described above. After washes, cells were incubated with 100 nM of unlabeled VEGFR2 (Sino Biological Inc., Beijing, China) for 30 min or 4 h, before incubation with labeled secondary antibody and HSA, as described above. Colonies from the fourth sorting round were analyzed by sequencing.

On-cell ranking of second-generation VEGFR2-binding Affibody molecules. Individual clones from the fourth sorting round that were selected for on-cell ranking were cultivated and labeled for flow-cytometry essentially as described above for the off-rate selection approach in the fourth sorting round, and analyzed using a Gallios flow cytometer (Beckman Coulter). Cells displaying first-generation binders Z_{VEGFR2_1} and Z_{VEGFR2_2} were included for comparison, and cells displaying a TNF-binding Affibody molecule were included as a negative control.

The top 10 ranked clones from $Z_{VEGFR2\_1matlib}$ and the top 8 ranked clones from $Z_{VEGFR2\_2matlib}$ were also analyzed for binding to murine VEGFR2, by labeling with mVEGFR2/Fc (R&D Systems), and analyzed using flow cytometry as described above. All experiments were performed in duplicates on different days using freshly prepared reagents.

Subcloning, expression and purification of second-generation binders. Four clones from $Z_{VEGFR2\_1matlib}$ (Z_{VEGFR2_11}, Z_{VEGFR2_16}, Z_{VEGFR2_19} and Z_{VEGFR2_22}) and four clones from $Z_{VEGFR2\_2matlib}$ (Z_{VEGFR2_33}, Z_{VEGFR2_38}, Z_{VEGFR2_41} and Z_{VEGFR2_40}) were sub-cloned to pET26-b(+), transformed to *E. coli* BL21 star (DE3) cells (Invitrogen), and soluble proteins were produced and purified as described above for the first generation binders Z_{VEGFR2_1} and Z_{VEGFR2_2}.

Circular dichroism analysis of second-generation VEGFR2-binding Affibody molecules. Circular dichroism experiments were performed as described previously[21].

Binding kinetics analysis of second-generation binders using surface plasmon resonance. Human VEGFR2/Fc was immobilized on a CM-5 sensor chip (GE Healthcare). Binding kinetics were analyzed by injecting different concentrations of the Affibody molecules (5, 10 and 20 nM) using a BIAcore™ 3000 instrument (GE Healthcare). Binding kinetics for Z_{VEGFR2_40} binding to murine VEGFR2 were determined using a BIAcore™ 3000 instrument (GE Healthcare) as described for human VEGFR2. For determination of the affinity constants of Z_{VEGFR2_22}, Z_{VEGFR2_19} and Z_{VEGFR2_16} for murine VEGFR2, the Affibody molecules were immobilized on a GLC sensor chip (Biorad Laboratories) using a ProteOn XPR36 instrument (Biorad Laboratories). 5, 10 and 20 nM murine VEGFR2 (Sino Biological) was injected over the surfaces. PBST 0.1 was used as a running buffer and 10 mM HCl for regeneration. The experiment was performed in duplicates using freshly prepared reagents.

SPR-based competition assay. Competition assays were performed essentially as described for the first-generation binders Z_{VEGFR2_1} and Z_{VEGFR2_2}. Details are provided in Supplementary Methods online.

Subcloning, expression and purification of dimer constructs. The genes encoding Z_{VEGFR2_22} and Z_{VEGFR2_40} were subcloned into the plasmid pET26b-Z_{02891}-ABD_{035}-Z_{Taq}[45] to generate four constructs: Z_{VEGFR2_22}-$(S_4G)_4$-ABD_{035}-$(S_4G)_4$-Z_{VEGFR2_40}, Z_{VEGFR2_40}-$(S_4G)_4$-ABD_{035}-$(S_4G)_4$-Z_{VEGFR2_22}, Z_{VEGFR2_22}-$(S_4G)_4$-ABD_{035}-$(S_4G)_4$-Z_{VEGFR2_22} and Z_{VEGFR2_40}-$(S_4G)_4$-ABD_{035}-$(S_4G)_4$-Z_{VEGFR2_40}. Subcloning and cultivation was performed as previously described[21].

Affibody molecules were purified using affinity chromatography with HSA immobilized on a sepharose matrix, and the buffer was exchanged to PBS using PD-10 columns (GE Healthcare, Uppsala, Sweden). The purity and size of the purified proteins were analyzed by SDS-PAGE and MALDI-time of flight (TOF) mass spectrometry using a LaserToF LT3 Plus instrument (SAI, Manchester, UK).

SPR analysis of dimeric Affibody constructs. The binding of the four dimeric constructs to human and murine VEGFR2 was analyzed by SPR. HSA (Sigma-Aldrich) was immobilized on a GLM sensor chip (Biorad Laboratories) using a ProteOn XPR36 instrument (Biorad Laboratories). The apparent dissociation constants (k_d) were estimated by injections of 200 nM of each of the homodimeric and heterodimeric constructs over the immobilized HSA, immediately followed by injections of 5, 15 and 45 nM human or murine VEGFR2 (for the heterodimers), or 15, 30 and 60 nM of human or murine VEGFR2 (for the homodimers). The dissociation constants were obtained from sensorgrams using a monovalent binding equation and non-linear regression. The experiment was performed in duplicates using freshly prepared reagents.

Cell-binding analysis. 293/KDR cells (Sibtech Inc., Brookfield, CT, USA) and HEK293 cells (ATCC, Manassas, VA, USA) were cultivated in Dulbecco's Modified Eagle Medium (DMEM, Sigma-Aldrich) supplemented with 10% fetal bovine serum (FBS), and (for 293/KDR) 2 mM L-glutamine. Cells growing on a petri dish were washed with PBS and harvested by pipetting. Cells were incubated for 20 min on ice with 500 nM of dimeric Affibody construct, the negative control construct Z_{Taq}-$(S_4G)_4$-ABD_{035}-$(S_4G)_4$-Z_{Taq} or the positive control mouse anti-hVEGFR2 IgG (R&D Systems), in PBS + 1% BSA (Sigma-Aldrich) (PBSB). Thereafter, cells were pelleted by centrifugation at 300 rpm for 4 min, and re-suspended in 150 nM HSA (Sigma-Aldrich) conjugated to Alexa Fluor 647 (Invitrogen). After incubation on ice in the dark for 20 min, cells were pelleted and re-suspended in PBSB, and analyzed using a Gallios flow cytometer (Beckman Coulter). The experiment was performed in duplicates using freshly prepared reagents.

Inhibition of VEGFR2 phosphorylation. 293/KDR cells (Sibtech Inc.) were cultured as described above, and seeded in DMEM (Sigma-Aldrich) supplemented with 10% FSB and 2 mM L-glutamine. 6 h after seeding, the medium was exchanged to starvation media (DMEM supplemented with 0.5% FBS), and cells were incubated overnight. Thereafter, cells were treated with 30 nM or 3 nM of the biparatopic binder Z_{VEGFR2_22}-$(S_4G)_4$-ABD_{035}-$(S_4G)_4$-Z_{VEGFR2_40}, a combination of 30 nM or 3 nM of each of the monomeric binders Z_{VEGFR2_22} and Z_{VEGFR2_40}, 30 nM or 3 nM of the negative control construct Z_{Taq}-$(S_4G)_4$-ABD_{035}-$(S_4G)_4$-Z_{Taq}, or PBS. After incubation for 1 h at 37°C, 1 nM human VEGF-A (R&D systems), or PBS, was added, and cells were incubated for 10 min at 37°C. Thereafter, cells were washed with PBS containing 1 mM sodium orthovanadate (Sigma), and scraped from the plate. Cell lysates were prepared by sonication for 1 min in Cell Lysis Buffer (Cell Signaling Technology, Danvers, MA, USA), supplemented with 1 mM sodium orthovanadate (Sigma) and 1 mM phenylmethylsulfonyl fluoride (PMSF, Sigma), and analyzed by ELISA using a PathScan® Phospho-VEGFR-2-Tyr1175 Sandwich ELISA kit (Cell Signaling Technology), according to the supplier's recommendations. The experiment was performed in duplicates.

1. Roskoski, R. Vascular endothelial growth factor (VEGF) signaling in tumor progression. *Critical reviews in oncology/hematology* **62**, 179–213, doi:10.1016/j.critrevonc.2007.01.006 (2007).

2. Tugues, S., Koch, S., Gualandi, L., Li, X. & Claesson-Welsh, L. Vascular endothelial growth factors and receptors: anti-angiogenic therapy in the treatment of cancer. *Mol Aspects Med* **32**, 88–111, doi:10.1016/j.mam.2011.04.004 (2011).
3. Hanahan, D. & Weinberg, R. A. The hallmarks of cancer. *Cell* **100**, 57–70 (2000).
4. Ferrara, N. Vascular endothelial growth factor: basic science and clinical progress. *Endocrine reviews* **25**, 581–611 (2004).
5. Muller, Y. A. *et al.* Vascular endothelial growth factor: crystal structure and functional mapping of the kinase domain receptor binding site. *P Natl Acad Sci USA* **94**, 7192–7197 (1997).
6. Brozzo, M. S. *et al.* Thermodynamic and structural description of allosterically regulated VEGFR-2 dimerization. *Blood* **119**, 1781–1788, doi:10.1182/blood2011-11-390922 (2012).
7. Matsui, J. *et al.* Multi-kinase inhibitor E7080 suppresses lymph node and lung metastases of human mammary breast tumor MDA-MB-231 via inhibition of vascular endothelial growth factor-receptor (VEGF-R) 2 and VEGF-R3 kinase. *Clin Cancer Res* **14**, 5459–5465, doi:10.1158/1078-0432.CCR-07-5270 (2008).
8. Polverino, A. *et al.* AMG 706, an oral, multikinase inhibitor that selectively targets vascular endothelial growth factor, platelet-derived growth factor, and kit receptors, potently inhibits angiogenesis and induces regression in tumor xenografts. *Cancer Res* **66**, 8715–8721, doi:10.1158/0008-5472.CAN-05-4665 (2006).
9. Wilhelm, S. M. *et al.* BAY 43-9006 exhibits broad spectrum oral antitumor activity and targets the RAF/MEK/ERK pathway and receptor tyrosine kinases involved in tumor progression and angiogenesis. *Cancer Res* **64**, 7099–7109, doi:10.1158/0008-5472.CAN-04-1443 (2004).
10. Mendel, D. B. *et al.* In vivo antitumor activity of SU11248, a novel tyrosine kinase inhibitor targeting vascular endothelial growth factor and platelet-derived growth factor receptors: determination of a pharmacokinetic/pharmacodynamic relationship. *Clin Cancer Res* **9**, 327–337 (2003).
11. Sullivan, L. A. & Brekken, R. A. The VEGF family in cancer and antibody-based strategies for their inhibition. *mAbs* **2**, 165–175 (2010).
12. He, K. *et al.* The effect of anti-VEGF drugs (bevacizumab and aflibercept) on the survival of patients with metastatic colorectal cancer (mCRC). *Onco Targets Ther* **5**, 59–65, doi:10.2147/OTT.S29719 (2012).
13. Potente, M., Gerhardt, H. & Carmeliet, P. Basic and therapeutic aspects of angiogenesis. *Cell* **146**, 873–887, doi:10.1016/j.cell.2011.08.039 (2011).
14. Sessa, C., Guibal, A., Del Conte, G. & Ruegg, C. Biomarkers of angiogenesis for the development of antiangiogenic therapies in oncology: tools or decorations? *Nat Clin Pract Oncol* **5**, 378–391, doi:10.1038/ncponc1150 (2008).
15. Lu, D. *et al.* Selection of high affinity human neutralizing antibodies to VEGFR2 from a large antibody phage display library for antiangiogenesis therapy. *Int J Cancer* **97**, 393–399 (2002).
16. Lu, D. *et al.* Tailoring in vitro selection for a picomolar affinity human antibody directed against vascular endothelial growth factor receptor 2 for enhanced neutralizing activity. *J Biol Chem* **278**, 43496–43507, doi:10.1074/jbc.M307742200 (2003).
17. Gagner, J. P., Law, M., Fischer, I., Newcomb, E. W. & Zagzag, D. Angiogenesis in gliomas: imaging and experimental therapeutics. *Brain Pathol* **15**, 342–363 (2005).
18. Price, S. J. & Gillard, J. H. Imaging biomarkers of brain tumour margin and tumour invasion. *Br J Radiol* **84 Spec No 2**, S159–167, doi:10.1259/bjr/26838774 (2011).
19. Choe, Y. S. & Lee, K. H. Targeted in vivo imaging of angiogenesis: present status and perspectives. *Curr Pharm Des* **13**, 17–31 (2007).
20. Olafsen, T. & Wu, A. M. Antibody vectors for imaging. *Semin Nucl Med* **40**, 167–181, doi:10.1053/j.semnuclmed.2009.12.005 (2010).
21. Malm, M. *et al.* Inhibiting HER3-Mediated Tumor Cell Growth with Affibody Molecules Engineered to Low Picomolar Affinity by Position-Directed Error-Prone PCR-Like Diversification. *PLoS ONE* **8**, doi:DOI 10.1371/journal.pone.0062791 (2013).
22. Orlova, A. *et al.* Tumor imaging using a picomolar affinity HER2 binding affibody molecule. *Cancer Res* **66**, 4339–4348, doi:10.1158/0008-5472.CAN-05-3521 (2006).
23. Behdani, M. *et al.* Development of VEGFR2-specific Nanobody Pseudomonas exotoxin A conjugated to provide efficient inhibition of tumor cell growth. *New biotechnology* **30**, 205–209, doi:10.1016/j.nbt.2012.09.002 (2013).
24. Tolcher, A. W. *et al.* Phase I and pharmacokinetic study of CT-322 (BMS-844203), a targeted Adnectin inhibitor of VEGFR-2 based on a domain of human fibronectin. *Clin Cancer Res* **17**, 363–371, doi:10.1158/1078-0432.CCR-10-1411 (2011).
25. Lofblom, J. *et al.* Affibody molecules: Engineered proteins for therapeutic, diagnostic and biotechnological applications. *FEBS Letters* **584**, 2670–2680, doi:10.1016/j.febslet.2010.04.014 (2010).
26. Sorensen, J. *et al.* First-in-human molecular imaging of HER2 expression in breast cancer metastases using the 111In-ABY-025 affibody molecule. *Journal of nuclear medicine: official publication, Society of Nuclear Medicine* **55**, 730–735, doi:10.2967/jnumed.113.131243 (2014).
27. Wallberg, H. & Orlova, A. Slow internalization of anti-HER2 synthetic affibody monomer 111In-DOTA-ZHER2:342-pep2: implications for development of labeled tracers. *Cancer Biother Radiopharm* **23**, 435–442, doi:10.1089/cbr.2008.0464 (2008).
28. Orlova, A., Tran, T. A., Ekblad, T., Karlstrom, A. E. & Tolmachev, V. (186)Re-maSGS-Z (HER2:342), a potential Affibody conjugate for systemic therapy of HER2-expressing tumours. *European journal of nuclear medicine and molecular imaging* **37**, 260–269, doi:10.1007/s00259-009-1268-9 (2010).
29. Wållberg, H., Ahlgren, S., Widström, C. & Orlova, A. Evaluation of the radiocobalt-labeled [MMA-DOTA-Cys61]-Z HER2:2395(-Cys) affibody molecule for targeting of HER2-expressing tumors. *Molecular imaging and biology: MIB: the official publication of the Academy of Molecular Imaging* **12**, 54–62, doi:10.1007/s11307-009-0238-8 (2010).
30. Tolmachev, V. *et al.* Imaging of EGFR expression in murine xenografts using site-specifically labelled anti-EGFR 111In-DOTA-ZEGFR:2377 Affibody molecule: aspect of the injected tracer amount. *European journal of nuclear medicine and molecular imaging* **37**, 613–622, doi:10.1007/s00259-009-1283-x (2009).
31. Kronqvist, N., Lofblom, J., Jonsson, A., Wernerus, H. & Stahl, S. A novel affinity protein selection system based on staphylococcal cell surface display and flow cytometry. *Protein Eng Des Sel* **21**, 247–255, doi:10.1093/protein/gzm090 (2008).
32. Jonsson, A., Dogan, J., Herne, N., Abrahmsen, L. & Nygren, P. A. Engineering of a femtomolar affinity binding protein to human serum albumin. *Protein Engineering Design and Selection* **21**, 515–527, doi:10.1093/protein/gzn028 (2008).
33. Kontermann, R. E. Strategies for extended serum half-life of protein therapeutics. *Current Opinion in Biotechnology* **22**, 868–876, doi:10.1016/j.copbio.2011.06.012 (2011).
34. Orlova, A. *et al.* Site-specific radiometal labeling and improved biodistribution using ABY-027, a novel HER2-targeting affibody molecule-albumin-binding domain fusion protein. *Journal of nuclear medicine: official publication, Society of Nuclear Medicine* **54**, 961–968, doi:10.2967/jnumed.112.110700 (2013).
35. Olsson, A. K., Dimberg, A., Kreuger, J. & Claesson-Welsh, L. VEGF receptor signalling - in control of vascular function. *Nat Rev Mol Cell Biol* **7**, 359–371, doi:10.1038/nrm1911 (2006).
36. Kronqvist, N. *et al.* Combining phage and staphylococcal surface display for generation of ErbB3-specific Affibody molecules. *Protein Eng Des Sel* **24**, 385–396, doi:10.1093/protein/gzq118 (2011).
37. Thiel, M. A. *et al.* Penetration of a topically administered anti-tumor necrosis factor alpha antibody fragment into the anterior chamber of the human eye. *Ophthalmology* **120**, 1403–1408, doi:10.1016/j.ophtha.2012.12.015 (2013).
38. LaFleur, D. W. *et al.* Monoclonal antibody therapeutics with up to five specificities: functional enhancement through fusion of target-specific peptides. *mAbs* **5**, 208–218, doi:10.4161/mabs.23043 (2013).
39. Yu, F. *et al.* An affibody-adalimumab hybrid blocks combined IL-6 and TNF-triggered serum amyloid A secretion in vivo. *mAbs* **6** 10.4161/mabs.36089 (2014).
40. Choi, H. J., Kim, Y. J., Lee, S. & Kim, Y. S. A heterodimeric Fc-based bispecific antibody simultaneously targeting VEGFR-2 and Met exhibits potent antitumor activity. *Mol Cancer Ther* **12**, 2748–2759, doi:10.1158/1535-7163.MCT-13-0628 (2013).
41. Shen, J. *et al.* Single variable domain-IgG fusion. A novel recombinant approach to Fc domain-containing bispecific antibodies. *J Biol Chem* **281**, 10706–10714, doi:10.1074/jbc.M513415200 (2006).
42. Papo, N., Silverman, A. P., Lahti, J. L. & Cochran, J. R. Antagonistic VEGF variants engineered to simultaneously bind to and inhibit VEGFR2 and αvβ3 integrin. *P Natl Acad Sci USA* **108**, 14067–14072, doi:10.1073/pnas.1016635108/-/DCSupplemental (2011).
43. Gronwall, C. *et al.* Selection and characterization of Affibody ligands binding to Alzheimer amyloid beta peptides. *Journal of Biotechnology* **128**, 162–183, doi:10.1016/j.jbiotec.2006.09.013 (2007).
44. Lofblom, J., Kronqvist, N., Uhlén, M., Stahl, S. & Wernerus, H. Optimization of electroporation-mediated transformation: Staphylococcus carnosus as model organism. *Journal of Applied Microbiology* **102**, 736–747, doi:10.1111/j.1365-2672.2006.03127.x (2007).
45. Malm, M. *et al.* Engineering of a bispecific affibody molecule towards HER2 and HER3 by addition of an albumin-binding domain allows for affinity purification and in vivo half-life extension. *Biotechnology journal*, doi:10.1002/biot.201400009 (2014).

Acknowledgments

This study was financially supported by the Swedish Foundation for Strategic Research (RBa08-0067) and the Swedish Research Council (2012-9975). Members of the Sel-tag Imaging Project (Q. Cheng, H. Wållberg, K. Johansson, H-S. Ahlzén, ESJ. Arnér, H. Lindberg, L. Lu, J-O. Thorell, E. Samén, M. Hägg, S. Linder, S. Nilsson, J. Grafström and S. Stone-Elander) are acknowledged for contributing to the experimental design and giving scientific advice.

Author contributions

F.F., S.K., E.G. and M.H. performed the experiments. F.F., S.K., E.G., F.Y.F., S.S. and J.L. contributed to experimental design. F.F., S.K., E.G., F.Y.F., S.S. and J.L. wrote the manuscript. All authors reviewed the manuscript.

Additional information

Supplementary information accompanies this paper at http://www.nature.com/scientificreports

Competing financial interests: SK, EG and FYF are employees at Affibody AB, Solna, Sweden. SS and JL are members of the Technical Advisory Board at Affibody AB. Other authors declare no financial or commercial conflict of interest.

How to cite this article: Fleetwood, F. *et al.* Simultaneous targeting of two ligand-binding sites on VEGFR2 using biparatopic Affibody molecules results in dramatically improved affinity. *Sci. Rep.* **4**, 7518; DOI:10.1038/srep07518 (2014).

This work is licensed under a Creative Commons Attribution-NonCommercial-NoDerivs 4.0 International License. The images or other third party material in this article are included in the article's Creative Commons license, unless indicated otherwise in the credit line; if the material is not included under the Creative Commons license, users will need to obtain permission from the license holder in order to reproduce the material. To view a copy of this license, visit http://creativecommons.org/licenses/by-nc-nd/4.0/